
Marginalising over Stationary Kernels with Bayesian Quadrature

Saad Hamid

Department of Engineering Science
University of Oxford
saad@robots.ox.ac.uk

Sebastian Schulze

Department of Engineering Science
University of Oxford
sschulze@robots.ox.ac.uk

Michael A. Osborne

Department of Engineering Science
University of Oxford
mosb@robots.ox.ac.uk

Stephen J. Roberts

Department of Engineering Science
University of Oxford
sjrob@robots.ox.ac.uk

Abstract

Marginalising over families of Gaussian Process kernels produces flexible model classes with well-calibrated uncertainty estimates. Existing approaches require likelihood evaluations of many kernels, rendering them prohibitively expensive for larger datasets. We propose a Bayesian Quadrature scheme to make this marginalisation more efficient and thereby more practical. Through use of the maximum mean discrepancies between distributions, we define a kernel over kernels that captures invariances between Spectral Mixture (SM) Kernels. Kernel samples are selected by generalising an information-theoretic acquisition function for warped Bayesian Quadrature. We show that our framework achieves more accurate predictions with better calibrated uncertainty than state-of-the-art baselines, especially when given limited (wall-clock) time budgets.

1 Introduction

Gaussian Processes (GPs) [1] are a rich class of models, which place probability distributions directly on classes of functions. Crucially, the success of these models is tied to the choice of their kernels. Analogously to architecture design in deep learning, kernels control the expressiveness and complexity of a GP model. If the correct kernel is chosen, GPs have shown the ability to make accurate predictions based on comparatively small training data sets. Beyond that, they natively provide predictive uncertainties with little additional computation. These confidence measurements are vital if model predictions form the basis for decision-making in the real world.

If, however, the chosen kernel is misspecified, little probability mass will be assigned to the neighbourhood of the true function, resulting in a poor fit. To increase model flexibility and avoid such pathologies practitioners typically define parameterised *kernel families* rather than specific kernels. The choice of a particular kernel is delayed until training and made data-dependent, e.g. via a maximum likelihood estimate (MLE).

Many commonly used kernels, such as the Radial Basis Function and Matérn kernels, have been shown to be universal kernels [2], meaning that they can approximate an arbitrary function in the limit of infinite data. However, in practice, the kernel choice encodes strong and frequently task-inappropriate inductive, significantly delaying learning progress. Performing inference over kernels therefore leads to better performance, particularly for large, complex data sets that exhibit complicated interactions between data points.

Our approach aims to create a flexible model capable of representing arbitrary stationary kernels and efficiently learning complex functions from large data sets. We draw on several previously separate strands of research to achieve this.

The analysis of kernels in the spectral domain has been shown to be an effective tool in learning expressive kernels [3]. Due to Bochner [4] a link between frequency densities and stationary kernel functions can be established. As a consequence posterior distributions over stationary kernels can be constructed from large data sets in a principled and computationally efficient way. This class of kernels is more general than previous manual constructions, requires little user intervention and is easily interpretable.

Rather than settling on a specific kernel via MLE, we conduct inference in the spectral-kernel framework by marginalising the entire kernel family against parameter likelihoods. The resulting integrals are computationally intractable and solutions can only be approximated. Previous approaches based on Markov chain Monte Carlo (MCMC) variants effectively average across likelihood evaluations of kernels randomly sampled from the posterior. Each likelihood evaluation requires an inversion of the kernel Gram matrix over all data points, making this approach increasingly expensive as we scale to larger data sets.

To stay efficient even in large data, expensive likelihood settings, we adopt a model-based approach to integral approximation. Bayesian Quadrature (BQ) [5, 6] methods model the function to be integrated directly. This allows for more careful sample acquisition, that yields performance superior to MCMC methods in wall-clock time for moderate-dimensional problems [7, 8].

Throughout this paper, we make the following contributions. Firstly, the construction of a custom *hyper*-kernel based on the maximum mean discrepancy between distributions. This kernel is cheap to evaluate, whilst producing meaningful covariances between spectral densities, regardless of their parameterisation. Secondly, a BQ framework based on this kernel to conduct computationally efficient inference on large data sets. Thirdly, the derivation of an information-theoretic acquisition function for the selection of new parameter evaluations. Finally, we empirically demonstrate the viability of the resulting approach on several synthetic examples and real world data sets. Our algorithm chooses informative likelihood evaluations and achieves high performance (log-likelihoods) on limited computational budgets measured in wall-clock time.

The societal impacts of this work will depend on the problems that practitioners apply it to, as it is a general-purpose framework.

2 Background

2.1 Gaussian Processes and their Covariance Functions

A Gaussian Process (GP) defines a probability distribution over the space of functions $f : \mathcal{X} \rightarrow \mathbb{R}$, such that for any finite subset $\mathcal{X}' \subset \mathcal{X}$, the vector $\{f(x)\}_{x \in \mathcal{X}'}$ is normally distributed. We denote such a distribution $f \sim \mathcal{GP}(m, k)$, where the mean $m(x) = E[f(x)]$ and kernel functions $k(x, x') = E[(f(x) - m(x))(f(x') - m(x'))]$ encode our prior beliefs about the function.

Analytic expressions for posterior mean and kernel of a process conditioned on a set of observations D under a Normal likelihood are readily available.¹

In the following kernels $k(x, x')$ are assumed to be part of the family of stationary kernels, taking the form²:

$$k(x, x') = k(x - x') = k(\rho), \quad (1)$$

such that two function values covary only depending on their separation and not their location.

Bochner’s Theorem [4] states that $k(\cdot)$ is a valid stationary covariance function on \mathbb{R} if and only if its Fourier transform, $S(\omega)$, is a positive finite measure over the frequency domain, i.e.:

$$k(\rho) = \int e^{2\pi i \rho \omega} S(\omega) d\omega. \quad (2)$$

¹We refer the interested reader to [1] for a detailed discussion of the GP framework.

²with slight abuse of notation.

For $k(\rho)$ to be real, we only consider symmetric $S(\omega)$. This creates an invertible mapping between a large subset of stationary kernels and the space of positive measures over frequencies. As a consequence, it is possible to parameterise the latter to induce a corresponding parameterisation of the former.

Kernels which take the form $k(x, y) = \exp(-\lambda d(x, y)^q)$ (λ being a hyper-parameter), are valid, i.e. positive definite, for $q = 1$ if and only if the underlying metric $d(x, y)$ is conditionally negative definite [9, 10], meaning that it must give rise to matrices, D , such that $c^T D c < 0, \forall c : \sum_i c_i = 0$. For $q = 2$ the underlying metric must be Hilbertian, meaning that there must be an isometry between the metric space defining d and a Hilbert space.

2.2 Bayesian Quadrature

Bayesian inference in machine learning frequently involves the computation of intractable integrals of the form:

$$Z = \int f(x)p(x)dx, \quad (3)$$

where $f(x)$ is a (likelihood-)function and $p(x)$ a prior density. Bayesian quadrature [5, 6] is a model-based approach to approximately evaluating such integrals by modelling f as a GP. Since GPs are closed under affine transforms the posterior over Z is then Gaussian. For some combinations of kernels and priors the quadrature weights can be evaluated analytically.

While the maintenance of the GP model requires some computational effort, this approach enables the generalisation of sample information across the integration domain. Consequently, samples can be chosen in a targeted fashion and BQ has been shown to be a competitive, more evaluation-efficient alternative to Monte Carlo methods, particularly in domains of moderate dimensionality.

Recent work [7, 8, 11] has proposed the use of warped GPs to further increase sample efficiency by encoding model-constraints such as the positivity of likelihood functions. This work builds upon WSABI [8] in particular, which places a GP prior over the square-root of the integrand. The acquisition function developed in Section 3.4 also applies to this setting and is an extension of the information-theoretic scheme discussed in Gessner et al. [12]. Osborne et al. [13] also proposed a BQ framework to infer ratios of integrals, which is relevant to the computation of marginalised posteriors. Additionally, the work of Xi et al. [14] and Chai et al. [15] is related as it concerns the use of BQ for computing correlated integrals, and for automatic model selection.

2.3 Gaussian Processes on Spaces of Measures

Recent work has used Wasserstein distances [16] to define Gaussian Processes on a space of measures. However, Wasserstein distances are only Hilbertian in 1D [17] so extensions to multidimensional distributions rely on Hilbert space embeddings of optimal transport maps to a reference distribution [18]. Furthermore, evaluating Wasserstein distances can be expensive as it involves finding the solution to an optimal transport problem. The Independence kernel based on the Sinkhorn distance [19] has been shown to be a valid positive definite kernel, but the distance between identical distributions may not be zero. Maximum mean discrepancies are defined in terms of kernel mean embeddings [20], so are Hilbertian.

2.4 Related work

Early work in kernel learning focussed on searching over compositions (sums and products) of a set of basic covariance functions [21]. More recent work has proposed learning kernels using their spectral representations [3, 22–32]. Beyond the ability to capture more complex structures, this approach also lends itself to approximate inference, reducing learning time complexity [24, 33, 34]. A model similar to ours uses a Dirichlet Process prior over the number of components in a Gaussian Mixture Model (GMM) residing in the spectral domain [26].

Inference in spectral models reduces to the marginalisation of the likelihood function against the posterior over kernels (or, equivalently, their spectral decompositions). The resulting integrals are intractable and have to be approximated – usually through the use of an appropriate MCMC scheme, such as Gibbs sampling, RJ-MCMC [35] or elliptical slice sampling [36]. Scaling MCMC marginalisation over the spectral kernel parameters up to large datasets is problematic. The computational

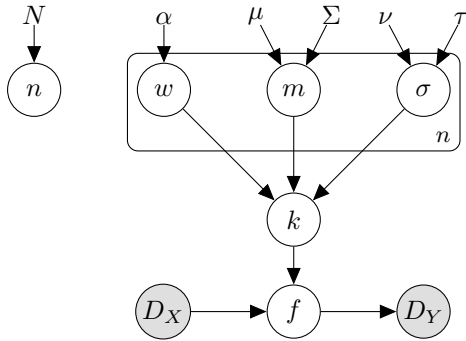


Figure 1: Bayesian Network of our model. The number of mixture components n is drawn from a uniform prior; α parameterises a Dirichlet distribution over the mixture weights w ; μ and Σ parameterise Gaussians over the mixture means; ν and τ parameterise Log-Normal distributions over the mixture scales. Not shown are the hyperparameters of the hyper-kernel, λ and l .

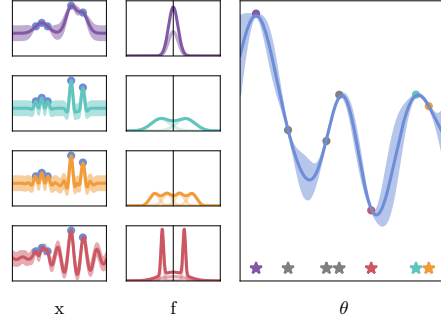


Figure 2: A schematic representation of the inference procedure under our model. The left column shows the GP posterior for different Spectral Mixture Kernels on the same dataset. The centre column shows the SM kernels in their spectral domain. The right column illustrates a GP posterior on a space indexed by the spectral densities of the SM kernels. BQ can then be used to marginalise over SM kernels which may have different numbers of mixture components.

cost of likelihood evaluations scales poorly in the size of the training data set and the collection of sufficiently many samples for an accurate Monte-Carlo estimate becomes prohibitively expensive. As above, BQ may be a more appropriate choice in these settings.

The BQ integrand model requires the specification of a positive-definite kernel across the integration domain – the space of spectral densities. While numerous metrics and divergences have been proposed to measure differences between probability distributions, many do not give rise to valid kernels. A notable exception is the maximum mean discrepancy, which is particularly efficient to calculate between Gaussian Mixture Models, a use case that will be of particular interest in this work.

The recently proposed baselines we will compare against include:

Variational Sparse Spectrum Gaussian Process (VSSGP) [24] which performs Variational Inference over a sparse spectrum approximation.

Bayesian Nonparametric Kernel Learning (BaNK) [26] which learns the posterior distribution over Spectral Mixture kernels via a Gibbs sampling scheme.

Functional Kernel Learning (FKL) [32] which places a GP prior over the kernel’s spectral density and infers a posterior over kernels using an Elliptical Slice Sampling scheme.

3 Our Method: MASKERADE

In this section, we introduce a flexible, data-efficient Gaussian Process regression model and show how to conduct inference within it.

3.1 A prior over spectral GMMs

Following Wilson and Adams [3] and Oliva et al. [26], we begin by parameterising spectral densities through the use of Gaussian mixture models. In the limit of infinitely many components GMMs can approximate any distribution to arbitrary precision. In practice, we limit the number of components to restrict the size of the parameter space. By Bochner’s theorem, a corresponding parameterisation of the space of stationary kernels can be obtained via the inverse Fourier Transform of a given GMM.

To perform Bayesian inference, we place a uniform prior over the number of mixture components n up to some maximum N and, for a given number of mixture components, Dirichlet priors over

weights w , normal priors over means m , and log-normal priors over the standard deviations σ (for details of the hyperpriors see Section 3.5). Note that the mixture is reflected at the origin to create only real-valued kernels. A graphical model of the resulting model is shown in Figure 1.

3.2 Inference

Under the above model, after observing data $\mathcal{D} = \{x_D, y_D\}$, the predictive distribution at x_* is given by:

$$p(y_* | x_*, D) = \frac{\sum_{n=1}^N \int p(y_* | x_*, \theta_n, D) p(D | \theta_n) p(\theta_n) d\theta_n}{\sum_{n=1}^N \int p(D | \theta_n) p(\theta_n) d\theta_n}, \quad (4)$$

where $\theta_n = \{w_i, m_i, \sigma_i\}_{i=1}^n$ are the parameters of an n -component GMM. The predictive distributions $p(y_* | x_*, \theta_n, D)$ and likelihoods $p(D | \theta_n)$ for a spectral kernel decomposition θ_n are given by the GP framework.

In Oliva et al. [26], Benton et al. [32], MCMC methods are used to sample spectral distributions S from the posterior and approximate the two integrals of interest simultaneously as averages of integrand evaluations. We note that each likelihood evaluation requires an inversion of the kernel Gram matrix of the entire data set and its computational cost increases quickly with data set size (typically cubically).

To reduce the number of likelihood evaluations needed to obtain a good approximation of the integrals of interest, we propose to adapt Bayesian Quadrature (BQ) approaches for their approximation.

Various approximations to reduce the cost of likelihood evaluations have been proposed in the literature, such as PCG [37] and BBMM [38] – modified conjugate gradient methods – and Random Fourier Features [33]. Our framework is optionally capable of leveraging both of these for scalability.

3.2.1 Bayesian Quadrature

We begin by constructing GP models of the functions $p(y_* | x_*, \theta_n, D) p(D | \theta_n)$ and $p(D | \theta_n)$ that are to be integrated against the prior. Since the locations x^* of test points are unknown at training time, inference separates into two steps.

During training, likelihood evaluations for a set of mixtures are collected (see Section 3.4), and the model evidences are computed. Following Gunter et al. [8] we enforce positivity of the likelihood surrogate by placing a GP prior over the square-root of the likelihood function $L(\theta_n) = P(D | \theta_n)$:

$$z = \sqrt{2(L(\theta_n) - \epsilon)} \sim \mathcal{GP}(0, k_{\text{spec}}), \quad (5)$$

where $k_{\text{spec}}(\theta_n, \theta_m)$ is a kernel between spectral densities (specifically GMMs parameterised by θ_n – see section 3.3) and ϵ is a small non-negative constant.

Under this model $L(\theta_n)$ is not a GP itself, but can be approximated as such using a linear transformation of the surrogate. In particular, the posterior mean and covariance functions $m_D^L(\theta_n)$ and $C_D^L(\theta_n, \theta_m)$ remain functions of the kernel k_{spec} and the likelihood observations. To ensure a good fit to the actual likelihood function, hyperparameters are re-optimised after each evaluation. Since GPs are closed under linear transformations, we obtain expressions for the first two moments of the model evidence integrals – those in the denominator of (4) – that are only composed of integrals of the kernel function and the prior. The model evidences are then given by $z^T W z$, where W are the BQ weights.

To make a prediction, we compute the integrals in the numerator of (4) in the same fashion. $p(y_* | x_*, \theta_n, D)$ is a GP posterior. Since we employ the same kernel k_{spec} to measure similarity between spectral densities, and we reuse the same likelihood evaluations from the training stage, the quadrature weights are identical and only z differs, allowing for efficient computation of the desired quantities. We note that the Bayesian Quadrature for Ratios framework outlined by Osborne et al. [13] could be adapted for use with WSABI. Unfortunately, this introduces further intractable integral terms, which must be approximated with Monte Carlo sampling, prohibitively raising the cost of inference.

3.3 The Hyper-Kernel

Noting that the densities under consideration are GMMs with a limited number of components, it becomes apparent that a suitable *hyper*-kernel, k_{spec} , has to overcome two obstacles. Firstly, it needs to cope with varying numbers of parameters, or otherwise assign a predefined covariance between GMMs with differing numbers of components. Secondly, it should capture a number of invariances in the parameterisation of GMMs (e.g. reordering of components, subdivision or recombination of components etc.). A naïve approach for the construction of such a kernel would base distances between densities on the Euclidean distance between their parameters and fails to achieve either desiderata. Instead, we seek a conditionally-negative definite or Hilbertian metric between distributions. The maximum mean discrepancy meets our criteria, and is cheap to compute.

We obtain the following kernel:

$$k_{\text{spec}}(\theta_n, \theta_m) = \lambda^2 \exp\left(-\frac{d(\theta_n, \theta_m)^q}{l^2}\right), \quad (6)$$

where $\lambda > 0$ is an output-scale, $l > 0$ is a length-scale parameter, $q = \{1, 2\}$ and d is a maximum mean discrepancy. The exact form of the MMD depends on the underlying kernel. Our experiments use the Energy Distance MMD, given by

$$d(\theta_n, \theta_m) = w_n^T M_{nm} w_m - \frac{1}{2} w_n^T M_{nn} w_n - \frac{1}{2} w_m^T M_{mm} w_m \quad (7)$$

where M_{nm} is a matrix of euclidean distances between all pairs of $\{(m_i, \sigma_i)\}_{i=1}^n$ and $\{(m_i, \sigma_i)\}_{i=1}^m$, but our framework allows for alternatives (e.g. the Gaussian MMD, which can also be computed analytically for GMMs). Note that, since the MMD is analytically computed (rather than approximated through sampling as is usual in the MMD literature), it is a valid distance between unnormalised densities. The hyper-kernel is therefore able to define covariances between kernels with arbitrary output-scales.

The only drawback is that integration of this kernel against the prior distribution is no longer possible analytically, so Monte Carlo integration is necessary. Arguably, however, the integration of the kernel against the prior lends itself better to such an approximation than that of the data likelihood. Intuitively, the likelihood function will have many sharp peaks for large datasets requiring samples to be drawn at very specific (unknown) locations for an accurate estimate. The kernel function by comparison is smoother, cheaper to evaluate and the resulting integral easier to approximate via random sampling from the prior. Our empirical results justify this approach, showing that we outperform competing methods despite the requirement for sampling.

3.4 Information-theoretic point acquisition

The GP surrogate is trained based on a set of sampled spectral distributions, $\mathcal{K} = \{(\theta_i, L_i)\}$, and the likelihood values of their corresponding kernels. Since adding a new point θ_n^{new} to this set requires a computationally expensive likelihood evaluation, it should be chosen to maximise its informativeness w.r.t. the quantity we care about – the predictive distribution at test locations x_* .

As we do not expect the model to have access to the test locations at training time, we choose a different acquisition criterion for the new point. Instead, we aim to improve the approximation of the denominator of (4) – and thereby the fit of the posterior distribution over spectral mixtures – at training time. In Gunter et al. [8] an acquisition function based on the uncertainty of the integrand is proposed. We extend the work of Gessner et al. [12] and Ru et al. [39] to propose an information-theoretic criterion instead.

We observe that the expected reduction in the entropy of our integral estimate after making an observation at sample location θ^s is given by:

$$\alpha(\theta^s) = H(L^s | \mathcal{K}, \theta^s) - E_{p(Z|\mathcal{K}, \theta^s)}[H(L^s | \mathcal{K}, \theta^s, Z)] \quad (8)$$

Here L^s is the predicted observation at location θ^s and Z is the sum of integrals in the denominator of (4). Within the GP framework, the entropy of the predictive distribution $H(L^s | \mathcal{K}, \theta^s)$ is the entropy of a Normal distribution and can be calculated in closed form. The second term turns out

to be the expectation of a constant and the predictive distribution conditioned on Z can once more be computed in closed form. Gessner et al. [12] discuss this acquisition function in the context of ordinary and multi-source Bayesian Quadrature. We note that it is available for warped Bayesian Quadrature. In particular, the acquisition function can be computed analytically when the linearisation approximation is used, provided that the kernel integrals are analytic. This is because the composition of the approximation and integration remains an affine transformation. Therefore, the integral of the approximate warped surrogate is jointly Gaussian distributed with the unwarped surrogate.

The acquisition function (8) is also valid for selecting batches of a fixed size. Importantly, our combination of hyper-kernel and acquisition function allows for the selection of (batches of) GMMs that are maximally informative about the sum of integrals, $\sum_{n=1}^N \int p(D | \theta_n) p(\theta_n) d\theta_n$, rather than selecting GMMs for each domain separately. This is because the kernel is able to define covariances between GMMs with different numbers of mixture components. Incorporating such information represents an improvement over Chai et al. [15] whose framework, in this instance, would be naïve as it assumes that the GPs over each domain are independent.

3.5 Hyperprior and Initialisation consideration

As with all Bayesian models, it is necessary to choose a suitable prior. We see this is an advantage to the practitioner, as they are able to include existing knowledge to reduce the space over which the integrand needs to be explored. In the absence of such information, we motivate a set of heuristic priors based on general properties of the training data (values in brackets were used in our experiments below).

The prior over the number of mixture components n is uniform up to maximum N ($N = 5$). The n components are weighted against one another through a dirichlet prior (concentration $\alpha = 1$). We normalise data sets by linearly scaling the input dimensions so that all training data lies in the interval $[0, 1]$, and shifting and scaling the outputs so that they have zero mean and unit variance.

Mixture means are drawn from a normal distribution with zero mean and standard deviation $F_s/5$ so that negligible mass lies above the Nyquist frequency F_s of the data. Recall that the Nyquist frequency is the highest frequency identifiable by a data set.

Mixture scales can be seen as approximate inverse lengthscales of the kernel. Accordingly their log-normal prior is set such that most of its mass lies between the inverse of the maximum distance between data points and the Nyquist frequency with a mean of $\log(1/|D_x|)$ and a scale of $\log(\sqrt{2})$ (where $|D_x|$ is the size of the data window).

Particularly, in large-scale data sets the likelihood surfaces are typically sparse. As a consequence, our GP model remains uninformative early on and the acquisition function is forced to explore the space under the prior until encountering high likelihood parameters. To avoid wasting computation on the optimisation of the acquisition function at this stage, we initialise our model with a set of parameters randomly drawn from the prior.

3.6 Computational Complexity

During learning, each iteration requires optimising the hyperparameters of the surrogate GP and the acquisition function. The time complexity of hyperparameter optimisation is dominated by the cost of making likelihood evaluations, $\mathcal{O}(l^2)$ where l is the number of Spectral Mixture kernels evaluated thus far. Acquisition function optimisation incurs an initial cost of $\mathcal{O}(l^3)$ to compute the cholesky decomposition of the hyper-kernel. Subsequent evaluations require $\mathcal{O}(bl^2)$ operations, where b is the batch size. The memory complexity of both parts of the algorithm are dominated by the cost of storing the hyper-kernel, $\mathcal{O}(l^2)$.

Once the evaluation budget is exhausted the quadrature weights can be computed in $\mathcal{O}(l^3)$. Inference takes $\mathcal{O}(l|D|^3)$ operations, though this can be reduced significantly by disregarding terms that have low quadrature weight. The memory complexity of inference is $\mathcal{O}(l^2|D|^2)$ for a naïve implementation, and can be reduced to $\mathcal{O}(l|D|^2)$ by looping appropriately (note that this leaves the asymptotic time complexity unchanged).

4 Results

In the following we empirically assess the performance of our model on a variety of tasks. We compare our approach of MARGinalising Spectral KERnels As DENSITIES (MASKERADE) to models previously proposed in the literature including VSSGP [24], BaNK [26], and FKL [32].

The experiments were conducted on a single Nvidia Titan V GPU. In all cases data is preprocessed so that the training targets have unit variance, and the training inputs lie in the range $[0, 1]$ in all dimensions. MASKERADE is parameterised to always marginalise over 5 spectral mixture components and select acquisitions in batches of 20.

4.1 Medium scale data sets

We begin by fitting MASKERADE to the Solar dataset [40] to compare against VSSGP. We replicate the setup from Gal and Turner [24], withholding 5 sets of length 20 as test sets. For this dataset, as with the others in this section, we allow MASKERADE 5 minutes for learning.

Table 1: Test set RMSE for the Solar Irradiance Data Set. Results for VSSGP are taken from Gal and Turner [24].

	VSSGP	MASKERADE
RMSE	0.41	0.17

We further examine the algorithms’ performance on four datasets from the UCI Machine Learning Repository [41]: Yacht Hydrodynamics (308 instances, 6 input dimensions) [42], Auto MPG (398 instances, 8 input dimensions) [43], Concrete Compressive Strength (1030 instances, 8 input dimensions) [44], and Airfoil Self-Noise (1503 instances, 5 input dimensions) [45].

To compare against FKL we follow Benton et al. [32] and average over 10 runs, randomly partitioning the data into 90/10 train/test sets every time. These results are presented in Table 2.

Table 2: Posterior log likelihood of and RMSE on the test set for UCI MLR datasets. Results for FKL taken from Benton et al. [32].

DATASET	LL		RMSE	
	FKL	MASKERADE	FKL	MASKERADE
YACHT	15.703 \pm 8.233	45.324 \pm 12.731	0.193 \pm 0.13	0.172 \pm 0.094
AUTOMPG	-98.942 \pm 6.135	-52.168 \pm 1.172	2.838 \pm 0.374	1.058 \pm 0.057
CONCRETE	-384.242 \pm 140.779	-145.41 \pm 55.84	3.781 \pm 0.501	0.719 \pm 0.145
AIRFOIL	-270.073 \pm 28.424	-135.09 \pm 15.76	1.378 \pm 0.176	0.565 \pm 0.104

Similarly, to compare against BaNK we follow Oliva et al. [26] and perform 3 repeats of 5-fold cross-validation on the Concrete Compressive Strength and Airfoil Self-Noise datasets, for which we present results in Table 3.

Table 3: Test set MSE on two UCI data sets. Results for BaNK taken from Oliva et al. [26].

DATASET	BANK	MASKERADE
CONCRETE	0.1195 \pm 0.0108	0.6889 \pm 0.0168
AIRFOIL	0.3359 \pm 0.0354	0.3244 \pm 0.0214

4.2 Large scale data sets

Finally we compare MASKERADE against FKL on two large datasets, with a limited time budget of 20 minutes for learning. We average over 10 runs with a 90/10 train/test split and report results in

Table 4. MASKERADE once more achieves superior performance to FKL on the same time budget. The datasets are the Sterling Broad Based Exchange Rate [46] (data from 1990-01-02–2020-10-08, totalling 7781 data points) and the UCI 3D Road Network [47] (10,000 data point subset of 250,000 data points. We choose the first 10,000 instances with a unique OSM-ID) for which the task is to predict altitude from latitude and longitude.

Table 4: Posterior log likelihood of and RMSE on the test set for FKL and MASKERADE fit to two large datasets. Both methods were given a time budget of 20 minutes for training.

DATASET	LL		RMSE	
	FKL	MASKERADE	FKL	MASKERADE
STERLING	-476.98 ± 342.94	162.34 ± 20.952	1.381 ± 1.011	1.132 ± 0.057
ROAD ALT	-3195.9 ± 68.029	-1102.4 ± 45.0945	5.809 ± 0.6478	0.729 ± 0.065

4.3 Ablation Study

We conduct an ablation study to verify the effectiveness of two components of our model in Table 5. Firstly, we verify that marginalising across the kernel family does indeed lead to better predictive performance. As a baseline, we compare against a GP using Spectral Mixture kernel (SM) whose hyperparameters were optimised via gradient descent to maximise the likelihood of the training data. Secondly, we compare our proposed acquisition function against uncertainty sampling [8] and random point acquisition. We set an evaluation budget of 1000 and evaluate performance on the Airline Passenger [48] and Mauna Loa Atmospheric CO₂ Concentration [49] datasets. We average over 10 runs with a 90/10 train/test split. In both cases, our chosen approach compares favourably to alternative designs.

5 Discussion

We have introduced a novel framework for kernel learning for Gaussian Processes that seeks to marginalise over Spectral Mixture Kernels using Bayesian Quadrature. Specifically we use a maximum mean discrepancy as a metric underlying an exponential kernel to define a Gaussian Process on a space of GMMs, and show how this can be efficiently computed. This elegantly incorporates invariances between Spectral Mixture Kernels into our model. Additionally we show that an information-theoretic acquisition function is applicable for warped Bayesian Quadrature, and how to use it within our framework. We empirically evaluate our method on several datasets and find that it is competitive with state-of-the-art baselines.

The key limitation of our method is due to the curse of dimensionality. The most scalable instantiation of our framework handles multi-dimensionality by using GMMs in which each Gaussian has a diagonal covariance structure. This means that the number of parameters for an SM kernel with M mixtures is $M(1 + 2D)$, which grows faster than the number of data dimensions, D . This limits the effectiveness of any Bayesian Quadrature regime, as the number of likelihood evaluations required to obtain a good estimate of the integrand becomes prohibitively large due to the cubic computational complexity. Note that Monte Carlo methods also suffer in high dimensional spaces, especially if likelihood evaluations are expensive. Our approach is most beneficial for inference based on large, low dimensional datasets.

Table 5: Test set RMSE for the Airline Passenger and Mauna Loa datasets. MASKERADE-I indicates the use of our proposed information theoretic acquisition function, MASKERADE-U indicates uncertainty sampling [8], and MASKERADE-R indicates random sampling under the prior.

DATASET	SM	MASKERADE-I	MASKERADE-U	MASKERADE-R
AIRPASS	0.283 ± 0.000	0.236 ± 0.044	0.274 ± 0.104	0.280 ± 0.140
MAUNA LOA	0.802 ± 0.685	0.243 ± 0.000	0.246 ± 0.126	0.360 ± 0.121

References

- [1] Carl Rasmussen and Christopher Williams. *Gaussian Processes for Machine Learning*. MIT Press, 2006.
- [2] Gabor Lugosi. Universal kernels. *Journal of Machine Learning Research*, 7:2651–2667, 2006.
- [3] Andrew Gordon Wilson and Ryan Prescott Adams. Gaussian Process Kernels for Pattern Discovery and Extrapolation. In *30th International Conference on Machine Learning*, pages 2104–2112, 2013.
- [4] Salomon Bochner. *Lectures on Fourier Integrals*, volume 42. Princeton University Press, 1959.
- [5] A. O’Hagan. Bayes–Hermite quadrature. *Journal of Statistical Planning and Inference*, 29(3): 245–260, 1991.
- [6] Carl Rasmussen and Zoubin Ghahramani. Bayesian monte carlo. In *Advanced in Neural Information Processing Systems 16*, 2003.
- [7] Michael A Osborne, David Duvenaud, Roman Garnett, Carl E Rasmussen, Stephen J Roberts, and Zoubin Ghahramani. Active learning of model evidence using Bayesian quadrature. In *Advances in Neural Information Processing Systems 26*, pages 46–54, 2012.
- [8] Tom Gunter, Michael A. Osborne, Roman Garnett, Philipp Hennig, and Stephen J. Roberts. Sampling for Inference in Probabilistic Models with Fast Bayesian Quadrature. In *Proceedings of the 28th Annual Conference on Neural Information Processing Systems*, volume 4, pages 2789–2797, 2014.
- [9] Sadeep Jayasumana, Richard Hartley, Mathieu Salzmann, Hongdong Li, and Mehrtash Harandi. Kernel Methods on Riemannian Manifolds with Gaussian RBF Kernels. *IEEE Transactions on Pattern Analysis and Machine Intelligence*, 37(12):2464–2477, 2015.
- [10] Aasa Feragen, Francois Lauze, and Søren Hauberg. Geodesic Exponential Kernels: When Curvature and Linearity Conflict. In *Proceedings of the IEEE Computer Society Conference on Computer Vision and Pattern Recognition*, pages 3032–3042, 2015.
- [11] Henry Chai and Roman Garnett. Improving Quadrature for Constrained Integrands. In *Proceedings of the 22nd International Conference on Artificial Intelligence and Statistics*, 2019.
- [12] Alexandra Gessner, Javier Gonzalez, and Maren Mahsereci. Active multi-information source bayesian quadrature. In Ryan P. Adams and Vibhav Gogate, editors, *Proceedings of The 35th Uncertainty in Artificial Intelligence Conference*, volume 115 of *Proceedings of Machine Learning Research*, pages 712–721, Tel Aviv, Israel, 22–25 Jul 2020. PMLR.
- [13] Michael A Osborne, Roman Garnett, Stephen J Roberts, Christopher Hart, Suzanne Aigrain, and Neale P Gibson. Bayesian quadrature for ratios. In *Proceedings of the 15th International Conference on Artificial Intelligence and Statistics*, pages 832–840, 2012.
- [14] Xiaoyue Xi, François-Xavier Briol, and Mark Girolami. Bayesian quadrature for multiple related integrals. In *35th International Conference on Machine Learning*, volume 12, pages 8533–8564, 2018. URL <http://arxiv.org/abs/1801.04153>.
- [15] Henry Chai, Jean-Francois Ton, Michael A Osborne, and Roman Garnett. Automated Model Selection with Bayesian Quadrature. In *36th International Conference on Machine Learning*, pages 1555–1564, 2019.
- [16] François Bachoc, Fabrice Gamboa, Jean-Michel Loubes, and Nil Venet. A Gaussian Process Regression Model for Distribution Inputs. *IEEE Transactions on Information Theory*, 64(10): 6620–6637, 2018.
- [17] Gabriel Peyré and Marco Cuturi. Computational Optimal Transport. *Foundations and Trends in Machine Learning*, 11(5):1–257, 2019.

- [18] Francois Bachoc, Alexandra Suvorikova, David Ginsbourger, Jean-Michel Loubes, and Vladimir Spokoiny. Gaussian processes with multidimensional distribution inputs via optimal transport and Hilbertian embedding. In *arXiv:1805.00753 [stat]*, 2019.
- [19] Marco Cuturi. Sinkhorn Distances: Lightspeed Computation of Optimal Transport. In *Advances in Neural Information Processing Systems 26*, pages 2292–2300, 2013.
- [20] Krikamol Muandet, Kenji Fukumizu, Bharath Sriperumbudur, and Bernhard Schölkopf. Kernel Mean Embedding of Distributions: A Review and Beyond. *Foundations and Trends in Machine Learning*, 10(1):1–141, 2017.
- [21] David Duvenaud, James Robert Lloyd, Roger Grosse, Joshua B. Tenenbaum, and Zoubin Ghahramani. Structure Discovery in Nonparametric Regression through Compositional Kernel Search. In *Proceedings of the 30th International Conference on Machine Learning*, 2013.
- [22] Yves-Laurent Kom Samo. *Advances in Kernel Methods*. PhD thesis, University of Oxford, 2017.
- [23] Miguel Lázaro-Gredilla, Joaquin Quiñero-Candela, Carl Edward Rasmussen, and Aníbal R Figueiras-Vidal. Sparse spectrum Gaussian process regression. *Journal of Machine Learning Research*, 11:1–17, 2010.
- [24] Yarin Gal and Richard Turner. Improving the Gaussian process sparse spectrum approximation by representing uncertainty in frequency inputs. In *32nd International Conference on Machine Learning*, volume 1, pages 655–664, 2015.
- [25] Yves-Laurent Kom Samo and Stephen Roberts. Generalized Spectral Kernels. In *arXiv:1506.02236 [stat]*, 2015.
- [26] Junier B Oliva, Avinava Dubey, Andrew G Wilson, Barnabas Poczos, Jeff Schneider, and Eric P Xing. Bayesian nonparametric kernel-learning. In *Proceedings of the 19th International Conference on Artificial Intelligence and Statistics*, pages 1078–1086, 2016.
- [27] Sami Remes, Markus Heinonen, and Samuel Kaski. Non-Stationary Spectral Kernels. In *Advances in Neural Information Processing Systems*, pages 4642–4651, 2017.
- [28] Phillip A Jang, Andrew Loeb, Matthew Davidow, and Andrew G Wilson. Scalable Levy Process Priors for Spectral Kernel Learning. In *Advanced in Neural Information Processing Systems*, pages 3941–3950, 2017.
- [29] Luca Ambrogioni and Eric Maris. Integral Transforms from Finite Data: An Application of Gaussian Process Regression to Fourier Analysis. In *Proceedings of the 21st International Conference on Artificial Intelligence and Statistics*, pages 217–225, 2018.
- [30] Felipe Tobar. Bayesian Nonparametric Spectral Estimation. In *Proceedings of the 32nd Conference on Neural Information Processing Systems*, 2018.
- [31] Tong Teng, Jie Chen, Yehong Zhang, and Kian Hsiang Low. Scalable Variational Bayesian Kernel Selection for Sparse Gaussian Process Regression. In *Proceedings of the 34th AAAI Conference on Artificial Intelligence*, 2019.
- [32] Gregory W. Benton, Wesley J. Maddox, Jayson P. Salkey, Julio Albinati, and Andrew Gordon Wilson. Function-Space Distributions over Kernels. In *Advanced in Neural Information Processing Systems*, 2019.
- [33] Ali Rahimi and Benjamin Recht. Random features for large-scale kernel machines. In *Advances in Neural Information Processing Systems 20*, pages 1177–1184. Curran Associates, Inc., 2008.
- [34] James Hensman, Nicolas Durrande, and Arno Solin. Variational Fourier features for Gaussian processes. *Journal of Machine Learning Research*, 18:1–52, 2018.
- [35] Peter J Green. Reversible jump markov chain monte carlo computation and Bayesian model determination. *Biometrika*, 82(4):711–732, 1995.

- [36] Iain Murray, Ryan Prescott Adams, and David J C MacKay. Elliptical slice sampling. *Journal of Machine Learning Research*, 9:541–548, 2010.
- [37] Kurt Cutajar, Michael Osborne, John Cunningham, and Maurizio Filippone. Preconditioning Kernel Matrices. In *International Conference on Machine Learning*, pages 2529–2538. PMLR, 2016.
- [38] Jacob R. Gardner, Geoff Pleiss, David Bindel, Kilian Q. Weinberger, and Andrew Gordon Wilson. GPyTorch: Blackbox Matrix-Matrix Gaussian Process Inference with GPU Acceleration. In *Advances in Neural Information Processing Systems*, 2018.
- [39] Binxin Ru, Mark McLeod, Diego Granziol, and Michael A. Osborne. Fast Information-theoretic Bayesian Optimisation. In *Proceedings of the 35th International Conference on Machine Learning*, 2018.
- [40] J. Lean. Solar Irradiance Reconstruction. IGBP PAGES/World Data Center for Paleoclimatology, Data Contribution Series # 2004-035. NOAA/NGDC Paleoclimatology Program, Boulder CO, USA, 2004. URL ftp://ftp.ncdc.noaa.gov/pub/data/paleo/climate_forcing/solar_variability/lean2000_irradiance.txt.
- [41] Dheeru Dua and Casey Graff. UCI Machine Learning Repository, 2017. URL <http://archive.ics.uci.edu/ml>.
- [42] Roberto Lopez. Yacht Hydrodynamics Data Set, 2013. URL <https://archive.ics.uci.edu/ml/datasets/yacht+hydrodynamics>.
- [43] Ross Quinlan. Auto MPG Data Set, 1993. URL <https://archive.ics.uci.edu/ml/datasets/auto+mpg>.
- [44] I-Cheng Yeh. Concrete Compressive Strength Data Set, 2007. URL <https://archive.ics.uci.edu/ml/datasets/concrete+compressive+strength>.
- [45] Roberto Lopez. Airfoil Self-Noise Data Set, 2014. URL <https://archive.ics.uci.edu/ml/datasets/airfoil+self-noise>.
- [46] Bank of England. Broad Effective Exchange Rate Index, Sterling, 2020. URL <https://www.quandl.com/data/BOE/XUDLBK82-Broad-Effective-Exchange-Rate-Index-Sterling-jan-2005-100>.
- [47] Manohar Kaul. 3D Road Network (North Jutland, Denmark) Data Set, 2013. URL [https://archive.ics.uci.edu/ml/datasets/3D+Road+Network+\(North+Jutland,+Denmark\)#](https://archive.ics.uci.edu/ml/datasets/3D+Road+Network+(North+Jutland,+Denmark)#).
- [48] S. Makridakis, S. Wheelwright, and R. Hyndman. Airline Passenger Data Set, 1998. URL <https://github.com/robjhyndman/fma/blob/master/data/airpass.rda>.
- [49] NOAA, USA. Mauna Loa Atmospheric CO₂ Observations, 2020. URL ftp://aftp.cmdl.noaa.gov/ccg/co2/trends/co2_mm_g1.csv.